Department of Social Systems and Management

Discussion Paper Series

No. 1175

Quadratic Ordered Median Location Problems

by

Yoshiaki OHSAWA, Naoya OZAKI, Frank PLASTRIA, and Kazuki TAMURA

July 2007

UNIVERSITY OF TSUKUBA
Tsukuba, Ibaraki 305-8573
JAPAN

Quadratic Ordered Median Location Problems

Yoshiaki OHSAWA
University of Tsukuba

Naoya OZAKI
Railway Technical Research Institute

Frank PLASTRIA
Vrije Universiteit Brussel

Kazuki TAMURA
Railway Technical Research Institute

November 24, 2006

Abstract The criteria used in location analysis have to be chosen according to the character of the facility. The single facility location models addressed in this paper accommodate simultaneous multiple criteria in a continuous space in the framework of ordered median problems, which generate and unify many standard location problems. We demonstrate that tools of computational geometry such as Voronoi diagrams and arrangements of curves and lines, enable us to identify the entire set of Pareto-optimal locations, when the squared Euclidean distances between the facility and affected inhabitants are used. For two objectives this works for any type of ordered median objectives and any polygonally bounded feasible region, but when more than two criteria are present the objectives and the feasible region have to be convex. In order to obtain this latter we use several recent structural results for unconstrained convex vector optimization, which we show to remain valid under a convex and compact constraint. Several examples illustrate our findings visually.

Keywords: location, multi-criteria, quadratic Euclidean distance, Pareto solutions, ordered median problem, Voronoi diagrams, arrangements of curves

1. Introduction

Recently, a great deal of effort has been spent on ordered median problems in continuous space, which considers the selection of the location of a facility. For example, rectilinear distance is incorporated in the framework of ordered median problems by Kalcsics et al.[14], Nickel and Puerto[17], Puerto and Fernández[30], Rodríguez-Chía et al.[31], Rodríguez-Chía and Puerto[32]. Euclidean distances in the framework of ordered median problems are used in Muñoz-Pérez and Saameño-Rodríguez[15]. A comprehensive and detailed overview of ordered median problems can be found in the recent book by Nickel and Puerto[16]. Ordered median problems are formulated in a quite general way to enhance their practical applicability. Many famous location problems can be regarded as special cases of this general model. Examples for attractive facilities are Weber problems, center problems and centdian problems. Examples for obnoxious facilities are anticenter problems and anti-Weber problems. Examples for equity facilities are minimization of range and mean-difference. On the other hand, there is a growing literature on multi-criteria approaches to optimize one or more than one objective functions in location analysis with remarkable corresponding progress in mathematical programming, as can be seen in the survey by Nickel et al.[18].

This paper provides a unified structure for the multi-criteria location model which is generated by combining continuous ordered median criteria with squared Euclidean distances. In fact, the two-objective models examined by Ohsawa[21], Ohsawa[22], Ohsawa et al.[23], Ohsawa et al.[24], Ohsawa and Tamura[25] can be regarded as special cases of our formulation. Their results are generalized and unified in the present framework using the subdivision of the feasible region into subregions where the objective function is either linear or quadratic. We consider explicitly a bounded feasible region, which is not only necessary to apply the models to practical problems but also to ensure that optimal locations for push objectives exists. We present the computational complexity in terms of the total input size, i.e. the number of fixed points and the number of edges of the feasible region.

Contrary to most existing planar location models, the research in this paper uses squared Euclidean distances, as in Ehrgott et al.[6], Fernández et al.[8], Francis and White[9], Ohsawa[21], Ohsawa et al.[23]. The main reason for choosing the squared Euclidean distance distances is that as far as their mathematical form is concerned, we can obtain analytical solutions for a lot of problems, while only few analytical results are available under Euclidean distance, even for the simple Weber problem. Another reason is that quadratic formulations generate simple circular level curves. This also enables us to have an easy geographical view similar to that obtained by a formulation using rectilinear distance, but without the disadvantage of axes dependency inherent in this latter. Thus, our formulation is quite useful to understand the essence of the ordered median problems.

First, we characterize the solution for *single-objective* ordered median problems based on a Voronoi diagram. Muñoz-Pérez and Saameño-Rodríguez[15] examined undesirable Euclidean ordered median problems, that is, the weights which are assigned to affected inhabitants according to the ordered distances are all negative. Our solution method relaxes this assumption in the sense that some weights can be positive and the others can be negative.

Next, we present a procedure to identify the Pareto set and its related trade-off curves for the *two-objective* problem generated by combining two types of ordered median criteria, which may be both neither convex nor concave. As pointed out by, for example, Das and Dennis[3], it is only under convexity assumptions that minimization of various convex combinations of the original criteria succeeds in obtaining the whole set of Pareto-optimal locations. In fact, Hamacher and Nickel[11] and Nickel and Puerto[17] devote their discussion to convex two-objective location problems, so they consider only restricted situations. We are able to overcome this difficulty through tools of computational geometry such as Voronoi diagrams and arrangements of curves and lines. We propose a solution method to solve *any* quadratic distance two-objective ordered median problem, even though each criterion and the feasible region might be non-convex.

Finally, we also develop an algorithm to produce all the two-dimensional Pareto-optimal locations associated with more than two convex ordered median criteria. To our knowledge, location models analytically dealing with more than two criteria are found only in Ehrgott et al.[6], Puerto and Fernández[28][29], Rodríguez-Chía and Puerto[32]. The first three works discuss only particular problems, while in the last work, only a generic algorithm is exhibited, while concrete code and its computational complexity are not stated. In contrast we describe fully an algorithm to generate the Pareto set for *any* quadratic distance convex ordered median problem together with its computational complexity.

The plan of the paper is as follows. We begin to study single-objective ordered median problems in Section 2. Section 3 is devoted to the two-objective models generated by combining two ordered median problems. Section 4 describes the multi-objective models, which are defined on a convex polygonal region by combining more than two convex ordered median criteria. Finally, Section 5 gives a number of concluding remarks.

2. Single-Objective Models

2.1. Problem formulation

Consider a bounded region Ω on a Euclidean plane where a facility can be built. We assume its boundary $\partial\Omega$ consists of a finite number $|\partial\Omega|$ of straight-line segments. Let I and $\{\mathbf{p}_1, \mathbf{p}_2, \ldots, \mathbf{p}_{|I|}\}$ be the index and location sets of the affected inhabitants on the plane, respectively. We will use a boldfaced letter to represent sites. Let $\|\cdot\|$ be the Euclidean norm. The weights $\alpha_1, \alpha_2, \cdots, \alpha_{|I|}$, which are assigned to the i-th nearest inhabitant from the facility, are given. They can be negative values.

We deal with the following *quadratic distance ordered median problem* to place a facility somewhere on the feasible region Ω:

$$\min_{\mathbf{x}\in\Omega} \left(F(\mathbf{x}) \equiv \sum_{i\in I} \alpha_i \|\mathbf{x} - \mathbf{p}_{(i)}\|^2 \right), \tag{1}$$

where (i) is the index of the i-th nearest point from $\mathbf{x}$ among $\{\mathbf{p}_1, \ldots, \mathbf{p}_{|I|}\}$, implying that the indices (i) depend on the location $\mathbf{x}$; the explicit dependence of the (i)'s on $\mathbf{x}$ is suppressed for notational simplicity. In location terminology, problem (1) seeks to minimize the sum of weighted quadratic Euclidean distances between the facility and inhabitants, depending on the order of the distances from $\mathbf{x}$. Table 1 is based on the summary table of Nickel and Puerto[16] and the examples presented in Muñoz-Pérez and Saameño-Rodríguez[15] and includes several new proposals. As suggested by the problems in Table 1, the ordered median location problem generalizes and unifies many standard location problems. As is instantly recognizable, if $\alpha_1 = \alpha_2 = \cdots = \alpha_{|I|} = 1$, then the ordered median problem (1) reduces to the well-known Weber criterion. If $\alpha_1 = \alpha_2 = \cdots = \alpha_{|I|} = -1$, problem (1) becomes the anti-Weber criterion. Therefore, the problems with $\alpha_i > 0$ for all $i \in I$ can be applied to desirable facilities, and those with $\alpha_i < 0$ for all $i \in I$ to undesirable facilities. On the other hand, if $\alpha_1 = -\alpha_{|I|} > 0$ and $\alpha_2 = \cdots = \alpha_{|I|-1} = 0$, then the problem (1) becomes the equity maximization using the range. Therefore, we see that the problem (1) is applicable to not only efficient location, but also to equity location.

Observe that when the set $\{\alpha_1, \alpha_2, \cdots, \alpha_{|I|}\}$ has only one nonzero element the problem (1) is equivalent to optimizing the corresponding objective function using simple Euclidean distance. Such problems are indicated by an asterisk in the second column of Table 1.

2.2. Properties

Voronoi diagrams are well studied concepts of Computational Geometry: see Okabe et al.[19], Ohyama[26]. Let $V_{i_1,i_2,\cdots,i_{|I|}}$ be the fully ordered Voronoi polygon associated with the sequence $\mathbf{p}_{i_1}, \mathbf{p}_{i_2}, \cdots, \mathbf{p}_{i_{|I|}}$. It can be mathematically expressed as

$$V_{i_1,i_2,\cdots,i_{|I|}} \equiv \{\mathbf{x} \in \mathbb{R}^2 \mid \|\mathbf{x}-\mathbf{p}_{i_1}\| \leq \|\mathbf{x}-\mathbf{p}_{i_2}\| \leq \cdots \leq \|\mathbf{x}-\mathbf{p}_{i_{|I|}}\|\}. \tag{2}$$

The *fully ordered Voronoi diagram* is defined by the union of all non-empty $V_{i_1,i_2,\cdots,i_{|I|}}$'s: see Ohsawa et al.[23]. This region is also called *ordered region* in Nickel and Puerto[16], Puerto and Fernández[30], Rodríguez-Chía et al.[31]. The cell-boundaries of this diagram coincide with the line tessellation generated by all the perpendicular bisectors of pairs $\mathbf{p}_i, \mathbf{p}_j$, which is explicitly used in Muñoz-Pérez and Saameño-Rodríguez[15]. This diagram contains all types of order Voronoi diagrams such as standard and farthest-point Voronoi diagrams as its subsets. Denote by ∂V the collection of the boundaries of $V_{i_1,i_2,\cdots,i_{|I|}}$'s within Ω.

Using the Voronoi region (2), $F(\mathbf{x})$ in (1) can be rewritten as

$$F(\mathbf{x}) \equiv \sum_{k\in I} \alpha_k \|\mathbf{x}-\mathbf{p}_{i_k}\|^2, \qquad \mathbf{x} \in V_{i_1,i_2,\cdots,i_{|I|}}. \tag{3}$$

If $\mathbf{x}$ is restricted to $V_{i_1,i_2,\cdots,i_{|I|}}$, then this problem becomes a squared Euclidean distance problem, as examined by Drezner and Wesolowsky[5]. Within $V_{i_1,i_2,\cdots,i_{|I|}}$ the indices i_k are independent of $\mathbf{x}$, contrary to (1).

Define A by $A \equiv \sum_{k\in I} \alpha_k$. When $A = 0$, we may rewrite (3) as

$$F(\mathbf{x}) = \langle\ \mathbf{x}\ ;\ \hat{\mathbf{p}}_{i_1,i_2,\cdots,i_{|I|}}\ \rangle + \sum_{k\in I} \alpha_k \|\mathbf{p}_{i_k}\|^2, \qquad \mathbf{x} \in V_{i_1,i_2,\cdots,i_{|I|}}, \tag{4}$$

where

$$\hat{\mathbf{p}}_{i_1,i_2,\cdots,i_{|I|}} \equiv -2\sum_{k\in I} \alpha_k \mathbf{p}_{i_k}. \tag{5}$$

Thus, $F(\mathbf{x})$ is piecewise linear, with contours within $V_{i_1,i_2,\cdots,i_{|I|}}$ being parallel lines orthogonal to $\hat{\mathbf{p}}_{i_1,i_2,\cdots,i_{|I|}}$.

When $A \neq 0$ an equivalent formulation of (3) is

$$F(\mathbf{x}) = A\|\mathbf{x}-\bar{\mathbf{p}}_{i_1,i_2,\cdots,i_{|I|}}\|^2 + \sum_{k\in I} \alpha_k \|\mathbf{p}_{i_k} - \bar{\mathbf{p}}_{i_1,i_2,\cdots,i_{|I|}}\|^2, \qquad \mathbf{x} \in V_{i_1,i_2,\cdots,i_{|I|}}, \tag{6}$$

where

$$\bar{\mathbf{p}}_{i_1,i_2,\cdots,i_{|I|}} \equiv \frac{1}{A}\sum_{k\in I} \alpha_k \mathbf{p}_{i_k} = -\frac{1}{2A}\hat{\mathbf{p}}_{i_1,i_2,\cdots,i_{|I|}}. \tag{7}$$

This calculation can be found in Francis and White[9]. Accordingly, it will be convenient to consider minimizing (when $A > 0$) or maximizing (when $A < 0$) $\|\mathbf{x}-\bar{\mathbf{p}}_{i_1,i_2,\cdots,i_{|I|}}\|^2$ rather than $F(\mathbf{x})$.

We have three remarks from the objective function (6). First, unless $A = 0$, the level sets of $F(\mathbf{x})$ within Voronoi polygon $V_{i_1,i_2,\cdots,i_{|I|}}$ are circular arcs concentric with respect to the center of gravity $\bar{\mathbf{p}}_{i_1,i_2,\cdots,i_{|I|}}$ and with a radius of

$$\sqrt{\frac{F(\mathbf{x}) - \sum_{k\in I} \alpha_k \left(\|\mathbf{p}_{i_k} - \overline{\mathbf{p}}_{i_1,i_2,\cdots,i_{|I|}}\|\right)^2}{|A|}}.$$

Second, mathematically if $A > 0$, then $F(\mathbf{x})$ is strictly convex within each Voronoi polygon, and if $A < 0$, then $F(\mathbf{x})$ is strictly concave within them. Thus, the sign of A plays an important role in simply and geometrically determining the region-wise functional forms. In addition, if $A > 0$ ($A < 0$), then $F(\mathbf{x})$ rises (falls) with the distance $\|\mathbf{x} - \overline{\mathbf{p}}_{i_1,i_2,\cdots,i_{|I|}}\|$. Therefore, in the context of facility planning, $F(\mathbf{x})$ with $A > 0$ may be regarded as a pull objective, and that $F(\mathbf{x})$ with $A < 0$ may be regarded as a push one. Some of the $F(\mathbf{x})$ with $A = 0$, e.g., range and mean difference, can be regarded as an equity criterion, as indicated in Table 1. The mean difference and the range are examined in Ohsawa et al.[23], Drezner et al.[4], respectively.

Finally, the function $F(\mathbf{x})$ is in general non-convex. As pictorially pointed out in Ohsawa et al.[24], partial center and partial anticenter problems can be non-convex. It is readily verified that the trimmed mean and range problems can be neither convex nor concave. However, if $0 \le \alpha_1 \le \alpha_2 \le \cdots \le \alpha_{|I|}$, then $F(\mathbf{x})$ is strictly convex, based on Crouzeix and Kebbour[2]. Thus, many pull objectives are strictly convex. The objective functions of mean difference and range are both convex. This is because they can be rewritten as $\sum_{i\in I}\sum_{j\in I} |\|\mathbf{x} - \mathbf{p}_i\|^2 - \|\mathbf{x} - \mathbf{p}_j\|^2|$ and $\max_{i,j\in I} |\|\mathbf{x} - \mathbf{p}_i\|^2 - \|\mathbf{x} - \mathbf{p}_j\|^2|$, respectively, and $|\|\mathbf{x} - \mathbf{p}_i\|^2 - \|\mathbf{x} - \mathbf{p}_j\|^2|$ is convex.

Define $\bar{P}$ as the set obtained by taking, for each permutation of the index set, the (unique) point of $V_{i_1,i_2,\cdots,i_{|I|}} \cap \Omega$ closest to $\bar{\mathbf{p}}_{i_1,i_2,\cdots,i_{|I|}}$, i.e., $\bar{\mathbf{p}}_{i_1,i_2,\cdots,i_{|I|}}$ itself or its nearest projection point on $V_{i_1,i_2,\cdots,i_{|I|}} \cap \Omega$.

Proposition 1 *If $A > 0$, then the minimum point of $F(\mathbf{x})$, denoted as $\mathbf{f}^*$, is located at $\bar{P}$. Otherwise, $\mathbf{f}^*$ is located at a vertex of $\partial V \cup \partial\Omega$.*

Proof If $A > 0$, then $F(\mathbf{x})$ is strictly convex on $V_{i_1,i_2,\cdots,i_{|I|}}$, so the constrained minimum $\mathbf{f}^*$ of $F(\mathbf{x})$ on $V_{i_1,i_2,\cdots,i_{|I|}} \cap \Omega$ is unique. The solution $\mathbf{f}^*$ is given by an element of the set $\bar{P}$. If $A \le 0$, then $F(\mathbf{x})$ is concave. This means that the optimal value of $F(\mathbf{x})$ on $V_{i_1,i_2,\cdots,i_{|I|}}$ will be reached at some extreme point of (the convex hull of) $V_{i_1,i_2,\cdots,i_{|I|}} \cap \Omega$. Such an extreme point is always a vertex of $\partial V \cup \partial\Omega$. ∎

Observe that concave vertices of Ω which are not on ∂V will never be an extreme point of any $V_{i_1,i_2,\cdots,i_{|I|}} \cap \Omega$, so should not be considered.

This proposition states that the optimal solutions are located at either $\bar{\mathbf{p}}_{i_1,i_2,\cdots,i_{|I|}}$ or $\partial V \cup \partial\Omega$. Our result contains the findings for partial center and partial anticenter problems formulated by Ohsawa et al.[24], and those for minimization problems of the mean-difference examined by Ohsawa et al.[23] as special cases. Our result is analogous to Theorem 4.5 of Nickel and Puerto[17] under rectilinear ordered median problems. The result for $\alpha_i < 0$ for all $i \in I$ is consistent with the finding using a simple Euclidean distance by Muñoz-Pérez and Saameño-Rodríguez[15].

2.3. Solution procedure

It follows from Proposition 1 that we may restrict our search to a finite set of candidate points, leading to the following method to obtain an optimal location:

Table 1: Quadratic single-objective ordered median problems

criterion	problem	weights$(\alpha_1, \alpha_2, \cdots, \alpha_{\lvert I\rvert})$	sign of A	convexity
pull	Weber	$(1, 1, \cdots, 1, 1)$	$+$	convex
	center*	$(0, 0, \cdots, 0, 1)$	$+$	convex
	k-centrum	$(0, \cdots, 0, \overbrace{1, \cdots, 1}^{k})$	$+$	convex
	cent-dian	$(\omega, \omega, \cdots, \omega, 1), \quad (0 \leq \omega \leq 1)$	$+$	convex
	partial center*	$(0, \cdots, 0, 1, \overbrace{0, \cdots, 0}^{n^+})$	$+$	—
	trimmed mean	$(\overbrace{0, \cdots, 0}^{m}, 1, \cdots, 1, \overbrace{0, \cdots, 0}^{m})$	$+$	—
push	anti-Weber	$(-1, -1, \cdots, -1, -1)$	$-$	concave
	anticenter*	$(-1, 0, \cdots, 0, 0)$	$-$	—
	anti-k-centrum	$(\overbrace{-1, \cdots, -1}^{k}, 0, \cdots, 0)$	$-$	—
	anticenter-maxian	$(-1, -\omega, \cdots, -\omega, -\omega), \quad (0 \leq \omega \leq 1)$	$-$	—
	partial anticenter*	$(\overbrace{0, \cdots, 0}^{n^-}, -1, 0, \cdots, 0)$	$-$	—
	anti-trimmed mean	$(\overbrace{0, \cdots, 0}^{m}, -1, \cdots, -1, \overbrace{0, \cdots, 0}^{m})$	$-$	—
equity	mean difference	$(1 - \lvert I\rvert, 3 - \lvert I\rvert, \cdots, \lvert I\rvert - 3, \lvert I\rvert - 1)$	0	convex
	range	$(-1, 0, \cdots, 0, 1)$	0	convex
	trimmed range	$(\overbrace{0, \cdots, 0}^{m}, -1, 0, \cdots, 0, 1, \overbrace{0, \cdots, 0}^{m})$	0	—

Algorithm 1

Step 1. Set up the planar graph $\partial V \cup \partial\Omega$.

Step 2. Find the minimum point of $F(\mathbf{x})$ from $\bar{P}$ (the nodes of the graph $\partial V \cup \partial\Omega$) for $A > 0$ ($A \leq 0$).

Proposition 2 *A solution* $\mathbf{f}^*$ *can be found in* $O(|I|^5 + |I|^3|\partial\Omega|)$ *time.*

Proof The graph $\partial V \cup \partial\Omega$ can be defined in $O(|I|^4 + |I|^2|\partial\Omega|)$ time, so Step 1 takes $O(|I|^4+|I|^2|\partial\Omega|)$. The graph has $O(|I|^4+|I|^2|\partial\Omega|)$ faces, and each center of gravity $\bar{\mathbf{p}}_{i_1,i_2,\cdots,i_{|I|}}$ can be identified in $O(|I|)$ based on (7). So all the nearest projection points can be identified in $O(|I|^5 + |I|^3|\partial\Omega|)$ time. There are $O(|I|^4 + |I|^2|\partial\Omega|)$ candidate points for the optimal solution. Using (3), each candidate can be evaluated in $O(|I|)$. Therefore, Step 2 can be done in $O(|I|^5 + |I|^3|\partial\Omega|)$, which equals the total time complexity. ∎

Note that if the feasible region Ω is convex, the complexity can be reduced to $O(|I|^5 + |I||\partial\Omega|)$ time, as shown in by Ohsawa et al.[23].

2.4. Computational experiments

We will illustrate the intuition behind our models by use of a real-world example. Suppose that Ibaraki Prefecture in Japan would construct one desirable and one undesirable facility within it to serve its inhabitants. The desirable facility is built based on the following k-centrum problem, which minimizes the sum of the squared Euclidean distances between the facility and the k farthest inhabitants: see Slater[33]. Its formulation is

$$\min_{\mathbf{x}\in\Omega}\left(\max_{\bar{I}\subseteq I,|\bar{I}|=k}\sum_{i\in\bar{I}}\|\mathbf{x}-\mathbf{p}_i\|^2\right).$$

A generalization of this objective is examined in Ogryczak and Tamir[20], Tamir[34].

The undesirable facility is constructed according to the anti-k-centrum problem, which is formulated in Muñoz-Pérez and Saameño-Rodríguez[15]. This problem is to maximize the sum of the distances between the facility and the k closest inhabitants as follows:

$$\max_{\mathbf{x}\in\Omega}\left(\min_{\bar{I}\subseteq I,|\bar{I}|=k}\sum_{i\in\bar{I}}\|\mathbf{x}-\mathbf{p}_i\|^2\right).$$

As indicated in Table 1, both problems belong to the quadratic ordered median problems. As special cases, if $k=|I|$, then the former problem reduces the quadratic distance variant of the well-known Weber problem, and the latter one reduces to the anti-Weber problem. If $k=1$, then the former problem reduces to the center problem, and the latter one reduces to the anti-center problem. We analyze how changing k affects optimal locations.

The location data of our example is shown in Figure 1. The affected points are eight municipalities with a population of more than 100,000 people in Ibaraki Prefecture on the first April, 2006. They are expressed as bullets in Figure 1. The fully ordered Voronoi diagram is also presented by lines. The optimal solutions $\mathbf{f}_k^*$ for the k-centrum problem, denoted as circles, are also given in this figure. The solution $\mathbf{f}_1^*$ coincides with the center, which is the circumcenter of Hitachi, Koga and Toride. The solution $\mathbf{f}_8^*$ has to be the center of gravity of those eight municipalities. We recognize from this figure that all the solutions are located in the central area of the prefecture, even though an increase in k changes slightly the solutions. Note that the solutions $\mathbf{f}_4^*$ and $\mathbf{f}_8^*$ are inner cell-points of V, and the others are on the boundary ∂V. ($\mathbf{f}_1^*$ and $\mathbf{f}_2^*$ are on the vertices of the boundary ∂V.)

The solutions $\mathbf{g}_k^*$ for the anti-k-centrum problem, denoted as triangles, are also shown in Figure 1. We see from this figure that the optimal solutions are restricted to only two places, and that the solution moves suddenly from the southeast corner of the prefecture to its northeast one as the parameter k is increased.

3. Two-Objective Models

3.1. Problem formulation

In addition to the ordered median problem (1), we consider another ordered median problem with weights $\beta_1,\beta_2,\cdots,\beta_{|I|}$:

$$\min_{\mathbf{x}\in\Omega}\left(G(\mathbf{x})\equiv\sum_{i\in I}\beta_i\|\mathbf{x}-\mathbf{p}_{(i)}\|^2\right). \tag{8}$$

In analogy to $\mathbf{f}^*$, A, $\hat{\mathbf{p}}_{i_1,i_2,\cdots,i_{|I|}}$ and $\bar{\mathbf{p}}_{i_1,i_2,\cdots,i_{|I|}}$, we define the notations $\mathbf{g}^*$, B, $\hat{\mathbf{q}}_{i_1,i_2,\cdots,i_{|I|}}$ and $\bar{\mathbf{q}}_{i_1,i_2,\cdots,i_{|I|}}$ for $G(\mathbf{x})$ similarly.

We consider the following *quadratic two-objective ordered median problem*, which is obtained by combining two types of ordered median problems (1) with (8):

$$\min_{\mathbf{x}\in\Omega}\{F(\mathbf{x}),G(\mathbf{x})\}. \tag{9}$$

The *Pareto-optimal locations* are simultaneously at least as good for both criteria, and strictly better for at least one criterion than any other feasible location. We call the set of all Pareto-optimal locations *Pareto set*, denoted as E^*. As in much of the multi-criteria literature, we state the location problem as a problem of deriving the Pareto set. As one moves along the Pareto set E^*, one can identify the subsequent trade-off curve between the extremes $\mathbf{f}^*$, $\mathbf{g}^*$ and all intermediate locations. Let $(F, G)(S) \equiv \{(F(\mathbf{x}), G(\mathbf{x}))|\mathbf{x} \in S\}$ for any set $S \subseteq \Omega$. We call $(F, G)(E^*)$ *trade-off curve* in the objective space.

As shown in Table 2, some special cases of our formulation (9) have already been investigated. An interesting special case of this formulation is the cent-dian problem: see Ohsawa[21]. Other interesting special cases are the partial anti-center and partial center problems, where both criteria are neither convex nor concave: see Ohsawa et al.[24].

In order to restrict the number of possibilities that need to be considered, some useless particular cases are eliminated by assuming that the points $\mathbf{p}_{i_1,i_2,\cdots,i_{|I|}}$ are in general position in the sense that

(a-1) any contour line of $F(\mathbf{x})$ intersects any contour line of $G(\mathbf{x})$ in isolated points only;
(a-2) both $F(\mathbf{x})$ and $G(\mathbf{x})$ have unique minimum solutions.

It follows from the assumption (a-1) that the Pareto set cannot contain two-dimensional areas. These assumptions are expressed mathematically by that for any $i_1, i_2, \cdots, i_{|I|}$,

(a-1)' if $AB \neq 0$, then $|A - B| + \|\bar{\mathbf{p}}_{i_1,i_2,\cdots,i_{|I|}} - \bar{\mathbf{q}}_{i_1,i_2,\cdots,i_{|I|}}\| \neq 0$, and if $|A| + |B| = 0$, then $c\hat{\mathbf{p}}_{i_1,i_2,\cdots,i_{|I|}} \neq \hat{\mathbf{q}}_{i_1,i_2,\cdots,i_{|I|}}$ for any constant $c(\neq 0)$;
(a-2)' $|A| + \|\hat{\mathbf{p}}_{i_1,i_2,\cdots,i_{|I|}}\| \neq 0$, and $|B| + \|\hat{\mathbf{q}}_{i_1,i_2,\cdots,i_{|I|}}\| \neq 0$.

It goes without saying that not all of these assumptions are needed for all results. In real applications using actual location data, our assumptions will almost always hold. Therefore, we can make these assumptions without loss of real-world applicability.

3.2. Properties

For each $V_{i_1,i_2,\cdots,i_{|I|}}$, we define the line $L_{i_1,i_2,\cdots,i_{|I|}}$ as follows:

$$L_{i_1,i_2,\cdots,i_{|I|}} = \begin{cases} \text{the line through } \bar{\mathbf{p}}_{i_1,i_2,\cdots,i_{|I|}} \text{ and } \bar{\mathbf{q}}_{i_1,i_2,\cdots,i_{|I|}}, & \text{if } AB \neq 0, \\ \text{the line through } \bar{\mathbf{q}}_{i_1,i_2,\cdots,i_{|I|}} \text{ in the direction } \hat{\mathbf{p}}_{i_1,i_2,\cdots,i_{|I|}}, & \text{if } A = 0 \text{ and } B \neq 0, \\ \text{the line through } \bar{\mathbf{p}}_{i_1,i_2,\cdots,i_{|I|}} \text{ in the direction } \hat{\mathbf{q}}_{i_1,i_2,\cdots,i_{|I|}}, & \text{if } A \neq 0 \text{ and } B = 0. \end{cases}$$

Define the line set L as the collection of $L_{i_1,i_2,\cdots,i_{|I|}}$ within $V_{i_1,i_2,\cdots,i_{|I|}} \cap \Omega$ for all permutations of the index sets with $V_{i_1,i_2,\cdots,i_{|I|}} \neq \phi$.

Proposition 3 *The Pareto set E^* is given by a subset of $\partial V \cup L \cup \partial\Omega$.*

Proof Unless a Pareto-optimal location is situated at the boundary of the Voronoi region $\partial V \cup \partial\Omega$, it must be a position where the contour of $F(\mathbf{x})$ and that of $G(\mathbf{x})$ are tangent. The former contour is either part of the circle with center at $\bar{\mathbf{p}}_{i_1,i_2,\cdots,i_{|I|}}$ or a linesegment orthogonal to $\hat{\mathbf{p}}_{i_1,i_2,\cdots,i_{|I|}}$. The latter is either a circular arc with center at $\bar{\mathbf{q}}_{i_1,i_2,\cdots,i_{|I|}}$ or a linesegment orthogonal to $\hat{\mathbf{q}}_{i_1,i_2,\cdots,i_{|I|}}$. Accordingly and because assumption (a-1), such a tangent position, i.e., the touching point of two contours, has to lie on a line segment $L_{i_1,i_2,\cdots,i_{|I|}}$. ∎

One may also observe more precisely that in case $AB > 0$, the candidates can be limited to the line segments connecting $\bar{\mathbf{p}}_{i_1,i_2,\cdots,i_{|I|}}$ and $\bar{\mathbf{q}}_{i_1,i_2,\cdots,i_{|I|}}$. When $AB < 0$ one may restrict search to the parts of the connecting lines outside these line segments. However, this detailed information does seem to be useful to reduce computational complexity. Proposition 3 states that we may restrict our search to the edges of the planar graph $\partial V \cup L \cup \partial\Omega$, indicating the noteworthy property that the Pareto set E^* has to be polygonal path.

Table 2: Quadratic two-objective ordered median problems

criteria	single-objective problems	convexity	reference
pull vs. pull	Weber vs. center	convex	[21]
pull vs. push	center vs. anti-center partial anti-center vs. partial center		[22] [24]
pull vs. equity	Weber vs. mean difference	convex	[23]
push vs. equity	anti-Weber vs. mean difference	concave	[23]

3.3. Solution procedure

Clearly, $\partial V \cup \partial\Omega \cup L$ may contain locations that cannot be Pareto-optimal. Accordingly, the Pareto set has still to be constructed within $\partial V \cup \partial\Omega \cup L$. The trade-off curve is given by the lower-left envelope of $(F,G)(\partial V \cup \partial\Omega \cup L)$. Hence, the Pareto set E^* and its corresponding trade-off curve can be specified by the following algorithm, which generalizes and unifies the methods by Ohsawa[21][22], Ohsawa et al.[23], Ohsawa et al.[24].

Algorithm 2

Step 1. Construct the planar graph $\partial V \cup L \cup \partial\Omega$.

Step 2. Delineate the loci of $(F,G)(\partial V \cup L \cup \partial\Omega)$ for the graph in objective space.

Step 3. Detect the lower-left envelope of the loci.

Step 4. Specify the parts which lie in the envelope in the geographical space.

Proposition 4 *The Pareto set* E^* *and the trade-off curve* $(F,G)(E^*)$ *can be found in* $O((|I|^4 + |I|^2|\partial\Omega|)(|I| + \log|\partial\Omega|)$ *time.*

Proof We can find the convex hull of Ω, denoted by $CH(\Omega)$ in $O(|\partial\Omega|\log|\partial\Omega|)$ time. By applying Step 1 of Algorithm 2 in Ohsawa et al.[23] for the convex hull $CH(\Omega)$, the graph $\partial V \cup L \cup \partial CH(\Omega)$ can be defined in $O(|I|^5 + |I||\partial\Omega|)$. We can cut off $\partial V \cup L \cup \Omega$ from $\partial V \cup L \cup \partial CH(\Omega)$, by traversing along $\partial\Omega$ in $O(|I|^2|\partial\Omega|)$. Thus, Step 1 has complexity $O((|I|^5 + |I|^2|\partial\Omega| + |\partial\Omega|\log|\partial\Omega|)$. Since the graph $\partial V \cup L \cup \partial\Omega$ has $O(|I|^4 + |I|^2|\partial\Omega|)$ edges, while using (3), Step 2 can be accomplished in $O(|I|^5 + |I|^3|\partial\Omega| + |\partial\Omega|\log|\partial\Omega|)$ time.

To define the envelope of the loci $(F,G)(\partial V \cup L \cup \partial\Omega)$, it is necessary to repeatedly identify where a pair of loci intersect. We consider the case of $AB \neq 0$. Let $\mathbf{p}'$ and $\mathbf{q}'$ be the projections of $\bar{\mathbf{p}}_{i_1,i_2,\cdots,i_{|I|}}$ and $\bar{\mathbf{q}}_{i_1,i_2,\cdots,i_{|I|}}$ onto a line l on $V_{i_1,i_2,\cdots,i_{|I|}}$, respectively. It follows from these definitions and equation (6) that for any location $\mathbf{x}$ on $l \cap V_{i_1,i_2,\cdots,i_{|I|}}$

$$
\begin{aligned}
F(\mathbf{x}) &= A\|\mathbf{x} - \mathbf{p}'\|^2 + C_1, & (10)\\
G(\mathbf{x}) &= B\|\mathbf{x} - \mathbf{q}'\|^2 + C_2, & (11)
\end{aligned}
$$

where

$$
\begin{aligned}
C_1 &\equiv A\|\mathbf{p}' - \bar{\mathbf{p}}_{i_1,i_2,\cdots,i_{|I|}}\|^2 + \sum_{k\in I}\alpha_k\|\mathbf{p}_{i_k} - \bar{\mathbf{p}}_{i_1,i_2,\cdots,i_{|I|}}\|^2,\\
C_2 &\equiv B\|\mathbf{q}' - \bar{\mathbf{q}}_{i_1,i_2,\cdots,i_{|I|}}\|^2 + \sum_{k\in I}\beta_k\|\mathbf{p}_{i_k} - \bar{\mathbf{q}}_{i_1,i_2,\cdots,i_{|I|}}\|^2.
\end{aligned}
$$

Parametrising the line l by $\mathbf{x} = (1-t)\mathbf{p}' + t\mathbf{q}'$, and eliminating t from the two equations (10) and (11), $G(\mathbf{x})$ can be exprssed as a quadratic function with respect to $F(\mathbf{x})$. This shows that two loci of the link within $(F,G)(\partial V \cup L \cup \partial\Omega)$ intersect each other at most twice. Thus, Step 3 requires $O((|I|^4 + |I|^2|\partial\Omega|)\log(|I|^4 + |I|^2|\partial\Omega|))$ time.

Since the graph $\partial V \cup L \cup \partial\Omega$ has $O(|I|^4 + |I|^2|\partial\Omega|)$ edges, the complexity of Step 4 is $O(|I|^4+|I|^2|\partial\Omega|)$. Noting that $O(|I|^5+|I|^3|\partial\Omega|+|\partial\Omega|\log|\partial\Omega|)+O((|I|^4+|I|^2|\partial\Omega|)\log(|I|^4+|I|^2|\partial\Omega|)) = O((|I|^4 + |I|^2|\partial\Omega|)(|I| + \log|\partial\Omega|))$, the proof is complete. ∎

Three notes are in order. First, if Ω is a convex region, the complexity can be reduced to $O((|I|^4+|\partial\Omega|)(|I|+\log|\partial\Omega|)$ time. Second, if $F(\mathbf{x})$ and $G(\mathbf{x})$ are both convex, an algorithm with lower computational complexity than Algorithm 2 may be established along the lines described in Ohsawa et al.[23]. This variant will also shortly be described in Section 4. Finally, Algorithm 2 runs, irrespective of convexity of two objective functions. Accordingly, the algorithm is applicable even to semi-obnoxious facility location, as examined by, for example, Carrizosa and Plastria[1].

3.4. Computational experiments

We consider two types of semi-obnoxious facility location which both focus on the trade-off between undesirable and desirable effects. For the sake of convenience, we use the location data with Ohsawa et al.[24], where there are only five affected points. The first is given as follows:

$$\min_{\mathbf{x}\in\Omega}\{F^1(\mathbf{x}), G^1(\mathbf{x})\}, \tag{12}$$

where,

$$F^1(\mathbf{x}) \equiv -\max_{\bar{I}\subseteq I, |\bar{I}|=|I|-2}\left(\min_{i\in\bar{I}}\|\mathbf{x}-\mathbf{p}_i\|^2\right), \tag{13}$$

$$G^1(\mathbf{x}) \equiv \sum_{i\in I}\|\mathbf{x}-\mathbf{p}_i\|^2 + \max_{i\in I}\|\mathbf{x}-\mathbf{p}_i\|^2. \tag{14}$$

The former criterion (13) is a partial anti-center problem, in which two inhabitants are neglected when determining facility location. Thus, the criterion seeks to maximize the nearest distance from the facility to $|I|-2$ inhabitants from an undesirable point of view. On the other hand, the latter criterion (14) is the cent-dian problem with the parameter $\omega = 0.5$ in Table 1. This is a classical two-objective problem for locating a desirable facility, whose idea is proposed by Halpern[10].

Next, we take up the following problem:

$$\min_{\mathbf{x}\in\Omega}\{F^2(\mathbf{x}), G^2(\mathbf{x})\}, \tag{15}$$

where,

$$F^2(\mathbf{x}) \equiv -\left(\sum_{i\in I}\|\mathbf{x}-\mathbf{p}_i\|^2 + \min_{i\in I}\|\mathbf{x}-\mathbf{p}_i\|^2\right), \tag{16}$$

$$G^2(\mathbf{x}) \equiv \min_{\bar{I}\subseteq I, |\bar{I}|=|I|-2}\left(\max_{i\in\bar{I}}\|\mathbf{x}-\mathbf{p}_i\|^2\right). \tag{17}$$

The former criterion (16) is an anti-center-maxion problem with the parameter $\omega = 0.5$ in Table 1, which is proposed in Eiselt and Laporte[7]. This is applicable for the determination of the location of an undesirable facility. On the other hand, the latter criterion (17) is the partial center problem, where two inhabitants are set aside for decision making. Thus, the criterion seeks to minimize the farthest distance from the facility to $|I|-2$ inhabitants from a desirable point of view.

Thus, in both problems (12) and (15), the facility location is determined based on the trade-off between desirable and undesirable powers. There are several notes. First, $F^1(\mathbf{x})$ and $G^2(\mathbf{x})$ are both non-concave and non-convex, although $G^1(\mathbf{x})$ is convex and $F^2(\mathbf{x})$ is concave. Second, the Pareto set associated with $F^1(\mathbf{x})$ and $G^2(\mathbf{x})$ is examined in Ohsawa et al.[24], where only two types of Voronoi diagrams are used, but here the line tessellation is necessary to solve the problem in order to use our solution method. This is because Weber and anti-Weber criteria are calculated on all the inhabitant location data.

Five affected points are indicated by $\mathbf{p}_i$'s. The graph $\partial V \cup L \cup \partial\Omega$ for the first two-objective problem (12) is delineated in Figure 2, where ∂V, L and $\partial\Omega$ are indicated by thin, broken and chain lines, respectively. The loci of $(F,G)(\partial V \cup L \cup \partial\Omega)$ are plotted in Figure 3 with the horizontal and vertical axes measuring values of F and G, respectively. As in Figure 2, the loci $(F,G)(\partial V)$, $(F,G)(L)$ and $(F,G)(\partial\Omega)$ are shown by thin, broken and chain lines, respectively. The lower envelope of the loci is indicated as solid curves. The corresponding Pareto set E^* is described by the solid locus in Figure 2. The set E^* consists of one isolated point, which is the minimizer of $G^1(\mathbf{x})$, i.e., $\mathbf{g}_1^*$, and two disconnected curve-segments. The optimal solution of $F^1(\mathbf{x})$, i.e., $\mathbf{f}_1^*$ is located at the endpoint of the bent segment. As is evident on referring to Figure 3, the trade-off curve $(F,G)(E^*)$, that is, the conflicts between the criteria F and G, is discontinuous. One part contains $(F,G)(\mathbf{f}_1^*)$, and another contains $(F,G)(\mathbf{g}_1^*)$.

Similarly, the graph $\partial V \cup L \cup \partial\Omega$ and the Pareto set E^* for the second two-objective problem (15) are delineated in Figure 4. The loci of $(F,G)(\partial V \cup L \cup \partial\Omega)$ and the trade-off curves $(F,G)(E^*)$ are depicted in Figure 5. The Pareto set comprises three polygonal paths. The optimal solutions of $F^2(\mathbf{x})$ and $G^2(\mathbf{x})$, denoted as $\mathbf{f}_2^*$ and $\mathbf{g}_2^*$, are located at one extreme of those paths. Contrary to Figure 3, the trade-off curve in Figure 5 is continuous between $(F,G)(\mathbf{f}_2^*)$ and $(F,G)(\mathbf{g}_2^*)$. A comparison of Figures 2 and 4 shows that the two Pareto sets are rather different, though the corresponding two two-objective problems are applicable to semi-obnoxious facility locations.

4. Convex Multicriteria Models

4.1. Problem formulation

In this section we consider that there are more than two convex quadratic ordered median criteria to be evaluated to determine the location of a facility on the feasible convex region Ω. Let Q be the index set of the quadratic ordered median criteria. So, $|Q|$ is the number of objectives. We will use superscript q to denote the q-th criteria for $q \in Q$. Here the following different quadratic convex ordered median problems are given:

$$\min_{\mathbf{x}\in\Omega} F^q(\mathbf{x}) \equiv \sum_{i\in I} \alpha_i^q \|\mathbf{x}-\mathbf{p}_{(i)}\|^2, \qquad q \in Q, \tag{18}$$

where $\alpha_1^q, \alpha_2^q, \cdots, \alpha_{|I|}^q$ are the weights for the q-th criterion. We define $A^q \equiv \sum_{i\in I} \alpha_i^q$. The convexity assumption then means that $A^q \geq 0$ for any $q \in Q$.

By combining these $|Q|$ single-objective problems in (18), we have the following *quadratic distance convex multi-criteria ordered median problem*:

$$\min_{\mathbf{x}\in\Omega} \left\{ F^1(\mathbf{x}), F^2(\mathbf{x}), \cdots, F^{|Q|}(\mathbf{x}) \right\}. \tag{19}$$

As before, we would like to construct the set of Pareto solutions E^* for (19), but this goal does not seem to be easily reachable directly in general. Instead, we will rather show how to construct the set of weak-Pareto solutions, i.e. the set of points $\mathbf{x} \in \Omega$ such that for any $\mathbf{y} \in \Omega$ we have $F^q(\mathbf{y}) \geq F^q(\mathbf{x})$ for some $q \in Q$. Under the mild condition that there cannot be equivalent solutions (i.e. when $F^q(\mathbf{y}) = F^q(\mathbf{x})$ for all $q \in Q$ implies $\mathbf{x} = \mathbf{y}$) these two sets coincide. In what follows we will assume that this holds. It is easy to see that this will be the case in particular when all the objectives $F^q(\mathbf{x})$ are strictly convex (i.e. $A_q > 0$), or when the points $\mathbf{p}_i$'s are in general position, in the following sense (extending the assumptions of previous section):

(b-1) contour lines of any two objectives intersect in isolated points only;

(b-2) all F^q have unique minimum solutions in Ω, denoted by $\mathbf{f}_q^*$.

Therefore the (weak) Pareto set for the problem (19) is still denoted as E^*. The Pareto set for the two-objective problem associated with $F^q(\mathbf{x})$ and $F^r(\mathbf{x})$ is likewise denoted as E^*_{qr}, while for the three-objective problem associated with $F^q(\mathbf{x})$, $F^r(\mathbf{x})$ and $F^s(\mathbf{x})$ it is denoted as E^*_{qrs}.

4.2. Properties

Consider the following unconstrained convex vector minimization problem:

$$\min_{\mathbf{x}\in\mathbb{R}^2} \left\{F^1(\mathbf{x}), F^2(\mathbf{x}), \cdots, F^{|Q|}(\mathbf{x})\right\}. \tag{20}$$

The following facts about the set of weak-Pareto solutions $WE(F^1, F^2, \cdots, F^{|Q|})$ for this unconstrained problem with inf-compact objectives (i.e. having compact lower level sets) defined on the plane $\mathbb{R}^2$ are known from literature:

(r-1) for two objectives: $WE(F^q, F^r)$ is a connected set connecting the minimal solutions $\mathbf{f}_q^*$ and $\mathbf{f}_r^*$ of each single objective problem. Under the assumptions made above it will be more precisely a continuous curve connecting these two points (see Hansen et al.[12]).

(r-2) for three objectives: $WE(F^q, F^r, F^s)$ is the part of the plane enclosed by the weak-Pareto sets of each two-objective sub-problem, $WE(F^q, F^r)$, $WE(F^r, F^s)$ and $WE(F^s, F^q)$, see Rodríguez-Chía and Puerto[32].

(r-3) for more than three objectives: we have (see Plastria and Carrizosa[27], Rodríguez-Chía and Puerto[32])

$$WE(F^1, F^2, \cdots, F^{|Q|}) = \bigcup_{Q'\subset Q, |Q'|=3} WE(F^q, q \in Q').$$

However, the same results hold also for such multiple objective problems constrained to some convex compact subset $S \subset \mathbb{R}^2$, as readily follows from the following technical lemma. The proof makes use of several notions and results of convex analysis, for which we refer in general to the book of Hiriart-Urruty and Lemaréchal [13]

Lemma 4.1 *Let S be a compact and convex subset of $\mathbb{R}^d$. Consider the constrained multi-objective problem (P):*

$$\min\{F^1, F^2, \cdots, F^{|Q|} | \mathbf{x} \in S\}$$

where all $F^q(\mathbf{x})$ are convex inf-compact functions defined on $\mathbb{R}^d$. Then one can find convex inf-compact functions $G^q(\mathbf{x})$ on $\mathbb{R}^d$, such that the (weak-)Pareto set for the unconstrained multi-objective problem (P'):

$$\min\{G^1, G^2, \cdots, G^{|Q|} | \mathbf{x} \in \mathbb{R}^d\}$$

equals the (weak-)Pareto set of (P).

Proof For every $q \in Q$ we will construct a convex inf-compact function $G^q(\mathbf{x})$ defined on $\mathbb{R}^d$, such that $G^q(\mathbf{s}) = F^q(\mathbf{s})$ for all $\mathbf{s} \in S$, and any point $\mathbf{x} \notin S$ is strictly dominated by some point $\mathbf{x}' \in S$, i.e. $G^q(\mathbf{x}) > G^q(\mathbf{x}') = F^q(\mathbf{x}')$. This will clearly prove the claimed result.

We may choose a compact $C \subset \mathbb{R}^d$ containing S in its interior. Since C is compact, each $F^q(\mathbf{x})$ is Lipschitz on C; call $L > 0$ a common strict Lipschitz constant for all $F^q(\mathbf{x})$ on C, i.e. for all $\mathbf{x} \neq \mathbf{y} \in C$ we have $F^q(\mathbf{x}) - F^q(\mathbf{y}) < L\|\mathbf{x} - \mathbf{y}\|$.

For every $F^q(\mathbf{x})$, each $\mathbf{a} \in S$ and each subgradient $\mathbf{p} \in \partial F^q(\mathbf{a})$, we may now consider the following function:

$$f_q^{\mathbf{a},\mathbf{p}}(\mathbf{x}) \equiv \langle\ \mathbf{x} - \mathbf{a}\ ;\ \mathbf{p}\ \rangle + F^q(\mathbf{a}).$$

By definition of subgradients we know that $f_q^{\mathbf{a},\mathbf{p}}(\mathbf{x}) \leq F^q(\mathbf{x})$ for all $\mathbf{x} \in \mathbb{R}^d$. If we choose in particular $\mathbf{x} = \mathbf{a} + \epsilon\mathbf{p}$ for some $\epsilon > 0$ sufficiently small to have $\mathbf{x} \in C$, we obtain $\epsilon\|\mathbf{p}\|^2 = \langle\ \mathbf{x} - \mathbf{a}\ ;\ \mathbf{p}\ \rangle \leq F^q(\mathbf{x}) - F^q(\mathbf{a}) < L\|\mathbf{x} - \mathbf{a}\| = L\epsilon\|\mathbf{p}\|$ from which we immediately obtain $\|\mathbf{p}\| < L$. Let us then define

$$H^q(\mathbf{x}) \equiv \sup_{\mathbf{a} \in S; \mathbf{p} \in \partial F^q(\mathbf{a})} f_q^{\mathbf{a},\mathbf{p}}(\mathbf{x})$$

which is well defined at all $\mathbf{x} \in \mathbb{R}^d$ because it is bounded above by $F^q(\mathbf{x})$. Note that we also have $H^q(\mathbf{s}) = F^q(\mathbf{s})$ for any $\mathbf{s} \in S$.

On the other hand we may define the function

$$J(\mathbf{x}) \equiv \sup_{\mathbf{b} \in bd\, S; \mathbf{q} \in N_S(\mathbf{b}) : \|\mathbf{q}\| = L} \langle\ \mathbf{x} - \mathbf{b}\ ;\ \mathbf{q}\ \rangle$$

which considers every boundary point $\mathbf{b} \in bd\, S$ combined with every vector $\mathbf{q}$ in the normal cone $N_S(\mathbf{b})$ of the convex set S at $\mathbf{b}$ with $\|\mathbf{q}\| = L$ (note that such $\mathbf{q}$ always exist). This supremum exists for any fixed $\mathbf{x} \in \mathbb{R}^d$ since it may be bounded above as follows: choose any fixed $\mathbf{s} \in S$ and let $R = \max_{\mathbf{b} \in bd\, S} \|\mathbf{s} - \mathbf{b}\|$ (which exists by compactness of $bd\, S$), then we have $\langle\ \mathbf{x} - \mathbf{b}\ ;\ \mathbf{q}\ \rangle \leq \|\mathbf{x} - \mathbf{b}\|\|\mathbf{q}\| \leq L(\|\mathbf{x} - \mathbf{s}\| + \|\mathbf{s} - \mathbf{b}\|) \leq L\|\mathbf{x} - \mathbf{s}\| + LR$. Note also that by definition of normal cone, for any $\mathbf{b} \in bd\, S$ and $\mathbf{q} \in N_S(\mathbf{b})$ we have that $\langle\ \mathbf{s} - \mathbf{b}\ ;\ \mathbf{q}\ \rangle \leq 0$ for all $\mathbf{s} \in S$, and therefore $J(\mathbf{s}) \leq 0$ for all $\mathbf{s} \in S$.

We now finally define for every $\mathbf{q} \in Q$ and $\mathbf{x} \in \mathbb{R}^d$

$$G^q(\mathbf{x}) = H^q(\mathbf{x}) + \max(0, J(\mathbf{x}))$$

and proceed by proving all the claimed properties of these functions.

First, as a pointwise supremum of affine functions, each $H^q(\mathbf{x})$ is convex on $\mathbb{R}^d$. For the same reason $J(\mathbf{x})$ is convex on $\mathbb{R}^d$, and therefore also $\max(0, J(\mathbf{x}))$. So $G^q(\mathbf{x})$ is a sum of convex functions, and therefore convex.

Second, let us show that $G^q(\mathbf{x})$ is inf-compact, for which it will be sufficient to prove that any lower level set $\{\mathbf{x} \in \mathbb{R}^d \mid G^q(\mathbf{x}) \leq K\}$ is bounded. To this end choose any fixed $\mathbf{a} \in S$. On the one hand, choosing any subgradient $\mathbf{p} \in \partial F^q(\mathbf{a})$, for which it was noted before that $\|\mathbf{p}\| < L$, we have $H(\mathbf{x}) \geq f_q^{\mathbf{a},\mathbf{p}}(\mathbf{x}) = \langle\ \mathbf{x} - \mathbf{a}\ ;\ \mathbf{p}\ \rangle + F^q(\mathbf{a}) \geq F^q(\mathbf{a}) - \|\mathbf{p}\|\|\mathbf{x} - \mathbf{a}\|$. On the other hand it is well-known that any $\mathbf{x} \notin S$ has a (unique) projection point $\mathbf{x}' \in S$, i.e. such that $\|\mathbf{x}' - \mathbf{x}\| \leq \|\mathbf{s} - \mathbf{x}\|$ for all $\mathbf{s} \in S$, and moreover $\mathbf{x}' \in bd\, S$ and $\mathbf{x}' - \mathbf{x} \in N_S(\mathbf{x}')$. Choosing $\mathbf{b} = \mathbf{x}'$ and $\mathbf{q} = L\frac{\mathbf{x}' - \mathbf{x}}{\|\mathbf{x}' - \mathbf{x}\|}$ we obtain $\langle\ \mathbf{x} - \mathbf{b}\ ;\ \mathbf{q}\ \rangle = L\|\mathbf{x}' - \mathbf{x}\|$, which proves that $J(\mathbf{x}) \geq L\|\mathbf{x}' - \mathbf{x}\| \geq L(\|\mathbf{x} - \mathbf{a}\| - \|\mathbf{x}' - \mathbf{a}\|)$. Summing we obtain $G^q(\mathbf{x}) \geq F^q(\mathbf{a}) - L\|\mathbf{x}' - \mathbf{a}\| + (L - \|\mathbf{p}\|)\|\mathbf{x} - \mathbf{a}\|$. Therefore, as soon as $G^q(\mathbf{x}) \leq K$ we have $\|\mathbf{x} - \mathbf{a}\| \leq \frac{K + LR - F^q(\mathbf{a})}{L - \|\mathbf{p}\|}$, which proves inf-compactness.

Third, for any $\mathbf{s} \in S$ we have already noted that $H^q(\mathbf{s}) = F^q(\mathbf{s})$ and $J(\mathbf{s}) \leq 0$, from which one immediately obtains $G^q(\mathbf{s}) = F^q(\mathbf{s})$.

Finally, let us show that any $\mathbf{x} \notin S$ is strictly dominated by its projection $\mathbf{x}'$ on S. Choosing $\mathbf{p} \in \partial F^q(\mathbf{x}')$, we have for every $q \in Q$, by definition of $H^q(\mathbf{x})$, that $H^q(\mathbf{x}) \geq f_q^{\mathbf{x}',\mathbf{p}}(\mathbf{x}) = \langle\, \mathbf{x}-\mathbf{x}' \,;\, \mathbf{p} \,\rangle + F^q(\mathbf{x}') \geq F^q(\mathbf{x}') - \|\mathbf{p}\|\|\mathbf{x}'-\mathbf{x}\|$. We saw above that $J(\mathbf{x}) \geq L\|\mathbf{x}'-\mathbf{x}\|$ and that $\|\mathbf{p}\| < L$, so we have

$$G^q(\mathbf{x}) \geq H^q(\mathbf{x}) + J(\mathbf{x}) \geq F^q(\mathbf{x}') + (L - \|\mathbf{p}\|)\|\mathbf{x}' - \mathbf{x}\| > F^q(\mathbf{x}') = G^q(\mathbf{x}')$$

which terminates the proof. ∎

For convex two-objective problems defined by $q, r \in Q$, the results of Section 3, writing now L^{qr} for the line set L defined there, show that the (weak) Pareto set E^*_{qr} consists of edges of the graph $\partial V \cup L^{qr} \cup \partial\Omega$. The additional information in the result (r-1), that for convex objectives E^*_{qr} forms a continuous curve joining $\mathbf{f}^*_q$ with $\mathbf{f}^*_r$, allows for the following direct determination of the line segments forming this curve, by generalization of the 'steepest descent path' idea pointed out in Ohsawa et al.[23].

Starting from $\mathbf{f}^*_q$, and later on more generally from some reached vertex $\mathbf{a}$ of the graph $\partial V \cup L^{qr} \cup \partial\Omega$, we have to choose which edge to follow in order to finally reach $\mathbf{f}^*_r$, and in this process the value of $F^r(\mathbf{x})$ must steadily decrease, while that of $F^q(\mathbf{x})$ must increase. Each edge incident with the vertex $\mathbf{a}$ will correspond to some curve in the $(F^q(\mathbf{x}), F^r(\mathbf{x}))$-diagram starting from $(F^q(\mathbf{a}), F^r(\mathbf{a}))$ and it is the non-dominated one we have to choose. Comparing with Figures 3 and 5 (where we measure $F^q(\mathbf{x})$ on the horizontal axis, and $F^r(\mathbf{x})$ on the vertical one) we see that this latter is the edge yielding the steepest downward slope in the $(F^q(\mathbf{x}), F^r(\mathbf{x}))$-diagram. Every edge incident with the vertex $\mathbf{a}$ is a line segment parallel to some direction $\mathbf{e} \neq \mathbf{0}$, and the slope of its (F^q, F^r)-image at $(F^q(\mathbf{a}), F^r(\mathbf{a}))$ equals the change of $F^r(\mathbf{x})$ relative to that of $F^q(\mathbf{x})$ when moving from $\mathbf{a}$ in the direction $\mathbf{e}$, which is given by the expression

$$\frac{DF^r(\mathbf{a})(\mathbf{e})}{DF^q(\mathbf{a})(\mathbf{e})} \tag{21}$$

where $DF^q(\mathbf{a})(\mathbf{e})$ denotes the directional derivative of $F^q(\mathbf{x})$ at the point $\mathbf{a}$ in the direction $\mathbf{e}$. Therefore at the vertex $\mathbf{a}$ we must always choose the edge of direction $\mathbf{e}$ that minimizes (21) among the $\mathbf{e}$ satisfying $DF^r(\mathbf{a})(\mathbf{e}) < 0$ and $DF^q(\mathbf{a})(\mathbf{e}) > 0$. In the exceptional case where the minimum is reached by several edges at $\mathbf{a}$, one can find the steepest direction by using the directional derivative of $F^q(\mathbf{x})$ of the second order at the point $\mathbf{a}$ because of $F^q(\mathbf{x})$ is quadratic. In what follows we will call the so constructed path the *steepest descent path from* $\mathbf{f}^*_q$ *to* $\mathbf{f}^*_r$.

Note finally that the directional derivatives are easy to calculate: each point $\mathbf{a}$ and edge, given by direction $\mathbf{e}$, to consider lies in (or on the boundary of) some region $V_{i_1,i_2,\cdots,i_{|I|}}$ in which the expressions (4) for $A^q = 0$ and (6) for $A^q > 0$ are valid, yielding

$$DF^q(\mathbf{a})(\mathbf{e}) = \begin{cases} \langle\, \mathbf{e} \,;\, \hat{\mathbf{p}}^q_{i_1,i_2,\cdots,i_{|I|}} \,\rangle, & \text{if } A^q = 0, \\ 2A^q\langle\, \mathbf{e} \,;\, \overline{\mathbf{p}}^q_{i_1,i_2,\cdots,i_{|I|}} - \mathbf{a} \,\rangle, & \text{if } A^q > 0, \end{cases}$$

where the definitions (5) and (7) are adapted to $F^q(\mathbf{x})$ by using the α^q_k's.

Proposition 5 *The Pareto set E^* consists of some connected faces of the planar graph $\partial V \cup \left(\bigcup_{q\in Q}\bigcup_{r\in Q,q>r} L^{qr}\right) \cup \partial\Omega$.*

Proof Combining the results (r-2) and (r-3) implies that the Pareto set E^* has to be enclosed by Pareto sets of type E^*_{qr}. This together with Proposition 3 means that E^* has to consist of connected faces of the planar graph $\partial V \cup \left(\bigcup_{q\in Q}\bigcup_{r\in Q,q>r} L^{qr}\right) \cup \partial\Omega$. ∎

Proposition 5 indicates that the Pareto set E^* has to be a polygonal region, whose boundary is given by edges of the fully ordered Voronoi diagram.

4.3. Solution procedure

Proposition 3 together with the proof of Proposition 5 yields the following algorithm to construct the geometrical description of the Pareto set E^* for the convex multi-criteria ordered median problem (19):

Algorithm 3

Step 1. Construct the planar graph $\partial V \cup \partial\Omega$, and identify the solutions $\mathbf{f}^*_q$'s for all $q \in Q$.

Step 2. For each q and $r(\neq q)$, define the planar graph $\partial V \cup L^{qr} \cup \partial\Omega$, and then find E^*_{qr}, i.e., the steepest descent path from $\mathbf{f}^*_q$ to $\mathbf{f}^*_r$ on $\partial V \cup L^{qr} \cup \partial\Omega$.

Step 3. For each q, r and s, find E^*_{qrs}, i.e., the area enclosed by E^*_{qr}, E^*_{rs} and E^*_{sq}.

Proposition 6 *Under the assumption of strict convexity or general position, the Pareto set E^* can be found in $O(|I|^5 + |I||\partial\Omega|)$ time.*

Proof Step 1 can be done in $O(|I|^5 + |I||\partial\Omega|)$ by applying Algorithm 1 for the convex region Ω, as noted in Section 2. For each pair of q and r, the graph $\partial V \cup L^{qr} \cup \partial\Omega$ can be established in $O(|I|^5 + |I||\partial\Omega|)$ time because Ω is convex, as implicitly noted in Section 3. Since there are $O(|I|^4 + |\partial\Omega|)$ edges in the graph, the steepest descent path can be found in $O(|I|^4 + |\partial\Omega|)$. Thus, Step 2 can be done in $O(|I|^5 + |I||\partial\Omega|)$. Since each steepest descent path has $O(|I|^4 + |\partial\Omega|)$ edges, the area enclosed by three paths can be determined in $O(|I|^4 + |\partial\Omega|)$. In conclusion, Algorithm 3 requires $O(|I|^5 + |I||\partial\Omega|)$. ∎

4.4. Computational experiments

For the sake of convenience, we use almost the same location data as Ohsawa et al.[23], shown in Figure 6, where five affected points are indicated as $\mathbf{p}_i$'s. The boundaries ∂V and $\partial\Omega$ are indicated by thin and chain lines, respectively. Here we examine the following four-objective problem

$$\min_{\mathbf{x}\in\Omega}\{F^1(\mathbf{x}), F^2(\mathbf{x}), F^3(\mathbf{x}), F^4(\mathbf{x})\}, \tag{22}$$

where

$$\begin{aligned}
F^1(\mathbf{x}) &\equiv \sum_{i\in I}\|\mathbf{x}-\mathbf{p}_i\|^2,\\
F^2(\mathbf{x}) &\equiv \sum_{i\in I}\sum_{j\in I}\left|\|\mathbf{x}-\mathbf{p}_i\|^2 - \|\mathbf{x}-\mathbf{p}_j\|^2\right|,\\
F^3(\mathbf{x}) &\equiv \max_{i\in I}\|\mathbf{x}-\mathbf{p}_i\|^2,\\
F^4(\mathbf{x}) &\equiv \max_{\bar{I}\subseteq I, |\bar{I}|=3}\left(\sum_{i\in\bar{I}}\|\mathbf{x}-\mathbf{p}_i\|^2\right).
\end{aligned}$$

The first and second criteria correspond respectively to Weber and minimization of mean difference problems. Hence they can be regarded as efficiency and equity criteria, respectively. The third is a simple center criterion, so it can be considered either as an efficiency or an equity criterion. As a fourth criterion, we consider the k-centrum problem with $k = 3$. As indicated in Table 1, these four criteria are all convex.

In order to solve the four-objective problem (22) according to Algorithm 3, first, following six two-objective sub-problems have to be separately solved:

$$\begin{array}{ll} \min\limits_{\mathbf{x}\in\Omega}\{F^1(\mathbf{x}), F^2(\mathbf{x})\}, & \min\limits_{\mathbf{x}\in\Omega}\{F^1(\mathbf{x}), F^3(\mathbf{x})\}, \\ \min\limits_{\mathbf{x}\in\Omega}\{F^1(\mathbf{x}), F^4(\mathbf{x})\}, & \min\limits_{\mathbf{x}\in\Omega}\{F^2(\mathbf{x}), F^3(\mathbf{x})\}, \\ \min\limits_{\mathbf{x}\in\Omega}\{F^2(\mathbf{x}), F^4(\mathbf{x})\}, & \min\limits_{\mathbf{x}\in\Omega}\{F^3(\mathbf{x}), F^4(\mathbf{x})\}. \end{array}$$

It should be noted that the first two problems are formulated in Ohsawa et al.[23] and in Ohsawa[21], respectively.

As shown in Figure 6, the optimal solutions $\mathbf{f}_1^*$, $\mathbf{f}_2^*$, $\mathbf{f}_3^*$ and $\mathbf{f}_4^*$ are located within the Voronoi polygon $V_{5,1,2,3,4}$.

Figures 7, 8, 9 and 10 give different increased views of Figure 6. Here the thick lines indicate the two-objective Pareto sets connecting the corresponding one-objective optimal points.

The Pareto set E_{12}^* (E_{13}^* and E_{23}^*) is given by the polygonal path from $\mathbf{f}_1^*$ to $\mathbf{f}_2^*$ through the point $\mathbf{v}$ (the polygonal path from $\mathbf{f}_1^*$ to $\mathbf{f}_3^*$ through the point $\mathbf{w}$, and the line between $\mathbf{f}_2^*$ and $\mathbf{f}_3^*$). The Pareto set E_{14}^* (E_{24}^* and E_{34}^*) is given by the edge between $\mathbf{f}_1^*$ and $\mathbf{f}_4^*$ (the polygonal path from $\mathbf{f}_2^*$ to $\mathbf{f}_4^*$ through the points $\mathbf{t}$ and $\mathbf{r}$, the polygonal path from $\mathbf{f}_3^*$ to $\mathbf{f}_4^*$ through the points $\mathbf{u}$ and $\mathbf{s}$). Note that the segment $\overline{\mathbf{f}_1^*\mathbf{v}}$ ($\overline{\mathbf{f}_1^*\mathbf{w}}$, $\overline{\mathbf{rt}}$, $\overline{\mathbf{st}}$) is a subset of L^{12}(L^{13}, L^{24}, L^{34}), and the segments $\overline{\mathbf{f}_1^*\mathbf{v}}$ and $\overline{\mathbf{rt}}$ are parallel to each other.

Second, based on the two-objective Pareto sets E_{12}^*, E_{13}^*, E_{14}^*, E_{23}^*, E_{24}^* and E_{33}^*, we can find the Pareto sets associated with each of the following four sub-problems:

$$\begin{array}{ll} \min\limits_{\mathbf{x}\in\Omega}\{F^1(\mathbf{x}), F^2(\mathbf{x}), F^3(\mathbf{x})\}, & \min\limits_{\mathbf{x}\in\Omega}\{F^1(\mathbf{x}), F^2(\mathbf{x}), F^4(\mathbf{x})\}, \\ \min\limits_{\mathbf{x}\in\Omega}\{F^1(\mathbf{x}), F^3(\mathbf{x}), F^4(\mathbf{x})\}. & \min\limits_{\mathbf{x}\in\Omega}\{F^2(\mathbf{x}), F^3(\mathbf{x}), F^4(\mathbf{x})\}. \end{array}$$

The Pareto set associated with $\min_{\mathbf{x}\in\Omega}\{F^1(\mathbf{x}), F^2(\mathbf{x}), F^3(\mathbf{x})\}$, which is enclosed by E_{12}^*, E_{13}^* and E_{23}^*, is given by the segment $\overline{\mathbf{f}_2^*\mathbf{t}}$, the segment $\overline{\mathbf{f}_3^*\mathbf{w}^*}$, and the triangle with vertices $\mathbf{f}_1^*$, $\mathbf{v}$, $\mathbf{w}$, as shown in Figure 7. As exhibited in Figure 8, the Pareto set E_{124}^* consists of the pentagon with vertices $\mathbf{f}_1^*$, $\mathbf{f}_4^*$, $\mathbf{r}$, $\mathbf{t}$, $\mathbf{v}$, and the segment $\overline{\mathbf{f}_2^*\mathbf{t}}$. Figure 9 shows that the set E_{134}^* is given by the pentagon with vertices $\mathbf{f}_1^*$, $\mathbf{f}_4^*$, $\mathbf{s}$, $\mathbf{u}$, $\mathbf{w}$, and the segment $\overline{\mathbf{f}_3^*\mathbf{w}}$. The Pareto set E_{234}^* is given by the quadrilateral with vertices $\mathbf{s}$, $\mathbf{r}$, $\mathbf{t}$, $\mathbf{u}$ and the three segments $\overline{\mathbf{f}_2^*\mathbf{t}}$, $\overline{\mathbf{f}_3^*\mathbf{u}}$ and $\overline{\mathbf{f}_4^*\mathbf{s}}$, as shown in Figure 10.

The shaded area displayed in Figure 6 is the union of E_{123}^*, E_{124}^*, E_{134}^* and E_{234}^* and gives the Pareto set E^*.

That is, the four-objective Pareto set is given by two segments $\overline{\mathbf{f}_2^*\mathbf{t}}$, $\overline{\mathbf{f}_3^*\mathbf{w}}$, and the pentagon with vertices $\mathbf{f}_1^*$, $\mathbf{f}_4^*$, $\mathbf{r}$, $\mathbf{t}$, $\mathbf{w}$.

Figure 6 clearly illustrates the well-known fact that the Pareto set expands as more criteria are used. For example, the optimal solution $\mathbf{f}_1^*$ is an element of the polygonal path E_{12}^*. This path is located within the Pareto area associated with E_{123}^*. This three-objective Pareto area is a subset of the four-objective Pareto area E^*.

5. Conclusions

Much attention has been given to ordered median location models, but relatively little to multi-objective formulations, in particular, non-convex cases. We present a polynomial-time algorithm to produce the Pareto-optimal solutions associated with many ordered median problems with the help of computational geometry such as Voronoi diagrams and arrangements of curves and lines. We devoted our discussion of ordered median problems to the squared Euclidean distances, but we expect that our results may quite easily be extended to other distances such as rectilinear distances, although more care will be needed in order to handle the difference between weak-Pareto and Pareto solutions.

Acknowledgment

This work was financed by the Research Grant of Japan Society for the Promotion of Science, Grant No. 18330057(2006).

References

[1] E. Carrizosa and F. Plastria: Location of semi-obnoxious facilities. *Studies in Locational Analysis*, 12(1999), 1–27.

[2] J.P. Crouzeix and R. Kebbour: On the convexity of some simple functions of ordered samples. *JORBEL: Belgian Journal of Operations Research, Statistics and Computer Sciences*, 36(1996), 11–25.

[3] I. Das and J. E. Dennis: A closer look at drawbacks of minimizing weighted sums of objectives for Pareto set generation in multicriteria optimization problems. *Structural Optimization*, 14(1997), 63–39.

[4] Z. Drezner, J.-F. Thisse and G.O. Wesolowsky: The minimax-min location problem. *Journal of Regional Science*, 26(1986), 87–101.

[5] Z. Drezner and G.O. Wesolowsky: The Weber problem on the plane with some negative weights. *INFOR*, 29(1991), 87–99.

[6] M. Ehrgott, H.W. Hamacher and S. Nickel: Geometric methods to solve max-ordering location problems. *Discrete Applied Mathematics*, 93(1999), 3–20.

[7] H.A. Eiselt and G. Laporte: Objectives in location problems. In Z. Drezner (ed.) *Facility Location: A Survey of Applications and Methods* (Springer, Berlin, 1995), 151–180.

[8] F.R. Fernández, S. Nickel, J. Puerto, and A. M. Rodriguez-Chia: Robustness in the Pareto-solutions for the multi-criteria minisum location problem. *Journal of Multi-Criteria Decision Analysis*, 10(2001), pp.191–203.

[9] R.K. Francis and J.A.White: *Facility Layout and Location: An Analytical Approach* (Prentice-Hall, Englewood Cliffs, 1974).

[10] J. Halpern: The location of a center-median convex combination on an undirected tree. *Journal of Regional Science*, 16(1976), 237–245.

[11] H.W. Hamacher and S. Nickel: Multicriteria planar location problems. *European Journal of Operational Research*, 94(1996), 66–86.

[12] P. Hansen, D. Peeters and J.-F. Thisse: Constrained location and the Weber-Rawls problem. *Annals of Operations Research*, 11(1981), 147–166.

[13] J.-B. Hiriart-Urruty and C. Lemaréchal: *Fundamentals of Convex Analysis* (Springer, Berlin, 2001).

[14] J. Kalcsics, S. Nickel, J. Puerto and A. Tamir: Algorithmic results for ordered median problems. *Operations Research Letters*, 30(2002), 149–158.

[15] J. Muñoz-Pérez and J.J. Saameño-Rodríguez: Location of an undesirable facility in a polygonal region with forbidden zones. *European Journal of Operational Research*, 114(1999), pp.372–379.

[16] S. Nickel and J. Puerto: A unified approach to network location problems. *Networks*, 34(1999), pp.283–290.

[17] S. Nickel and J. Puerto, *Location Theory –A Unified Approach–* (Springer, Berlin, 2005).

[18] S. Nickel, J. Puerto and A.M. Rodríguez-Chía: MCDM location problems. In J. Figueira, S. Greco and M. Ehrgott (eds.) *Multiple Criteria Decision Analysis* (Springer, New York, 2005), 761–795.

[19] A. Okabe, B. Boots, K. Sugihara and S.N. Chiu, *Spatial Tessellations* (Wiley, New York, 1999).

[20] W. Ogryczak, and A. Tamir: Minimizing the sum of the K largest functions in linear time. *Information Processing Letters*, 85(2003), pp.117–122.

[21] Y. Ohsawa: A geometrical solutions for quadratic bicriteria location models. *European Journal of Operational Research*, 114(1999), 380–388.

[22] Y. Ohsawa: Bicriteria Euclidean location associated with maximin and minimax criteria. *Naval Research Logistics*, 47(2000), 581–592.

[23] Y. Ohsawa, N.Ozaki and F.Plastria: Equity-Efficiency Bicriteria location with squared Euclidean distances. *Operations Research*, (2007), to appear.

[24] Y. Ohsawa, F.Plastria and K. Tamura: Euclidean push-pull partial covering problems. *Computers and Operations Research*, 33(2006), 3566–3582.

[25] Y. Ohsawa and K. Tamura, Efficient location for a semi-obnoxious facility: *Annals of Operations Research*, 123(2003), 173–188.

[26] T. Ohyama: Some Voronoi diagrams that consider consumer behavior analysis. *Japan Journal of Industrial and Applied Mathematics*, 22(2005), pp.279–290.

[27] F.Plastria and E.Carrizosa: Geometrical characterization of weakly efficient points. *Journal of Optimization Theory and Applications*, 90(1996), pp.217–223.

[28] J. Puerto and F.R. Fernández: A convergent approximation scheme for efficient sets of the multi-criteria Weber location problem. *Top*, 6(1998), pp.195–204.

[29] J. Puerto and F.R. Fernández: Multi-criteria minisum facility location problems. *Journal of Multi-Criteria Decision Analysis*, 8(1999), pp.268–280.

[30] J. Puerto and F.R. Fernández: Geometrical properties of the symmetrical single facility location problem. *Journal of Nonlinear and Convex Analysis*, 1(2000), pp.321–342.

[31] A.M. Rodríguez-Chía, S. Nickel, J. Puerto, and F.R. Fernández: A flexible approach to location problems. *Mathematical Methods of Operations Research*, 51(2000), pp.69–89.

[32] A.M. Rodríguez-Chía, and J. Puerto: Geometrical description of the weakly efficient solution set for multicriteria location problems. *Annals of Operations Research*, 111(2002), pp.181–196.

[33] P.J. Slater: Centers to centroids in graphs. *Journal of Graph Theory*, 2(1978), pp.209–222.

[34] A. Tamir: The k-centrum multi-facility location problem. *Discrete Applied Mathematics*, 109(2001), pp.293–307.

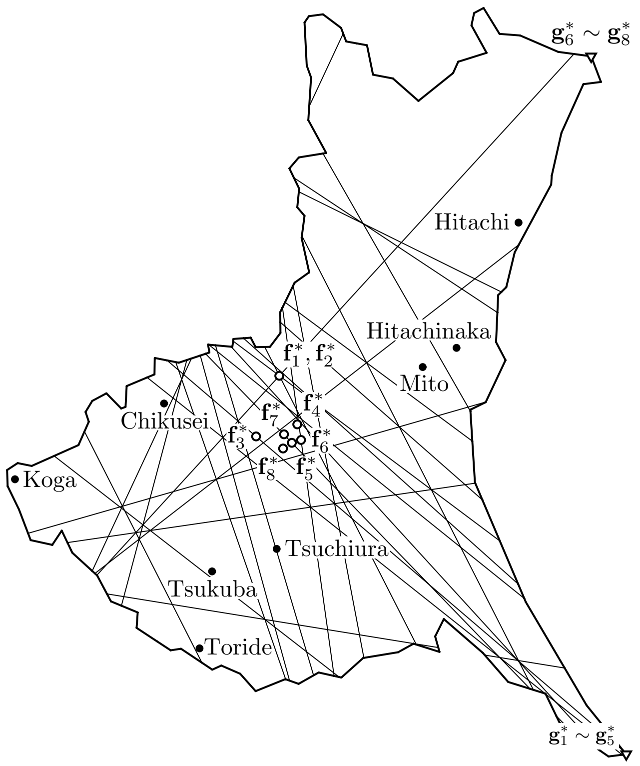

Figure 1: Graph $\partial V \cup \partial\Omega$ and solutions $\mathbf{f}_i^*$'s, $\mathbf{g}_i^*$'s

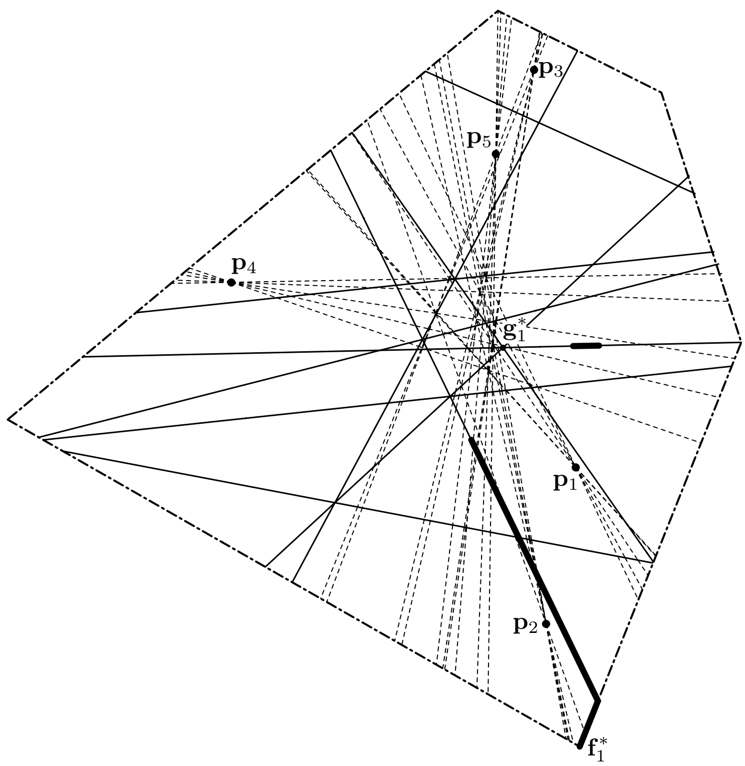

Figure 2: Pareto set for partial anticenter with cent-dian criteria

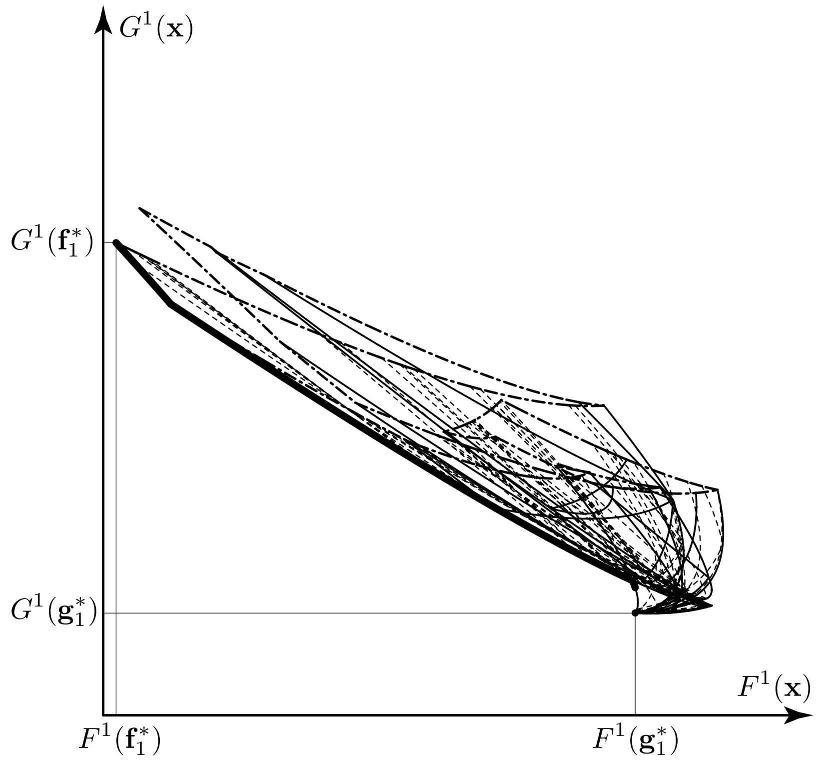

Figure 3: Trade-off curve for partial anticenter with cent-dian criteria

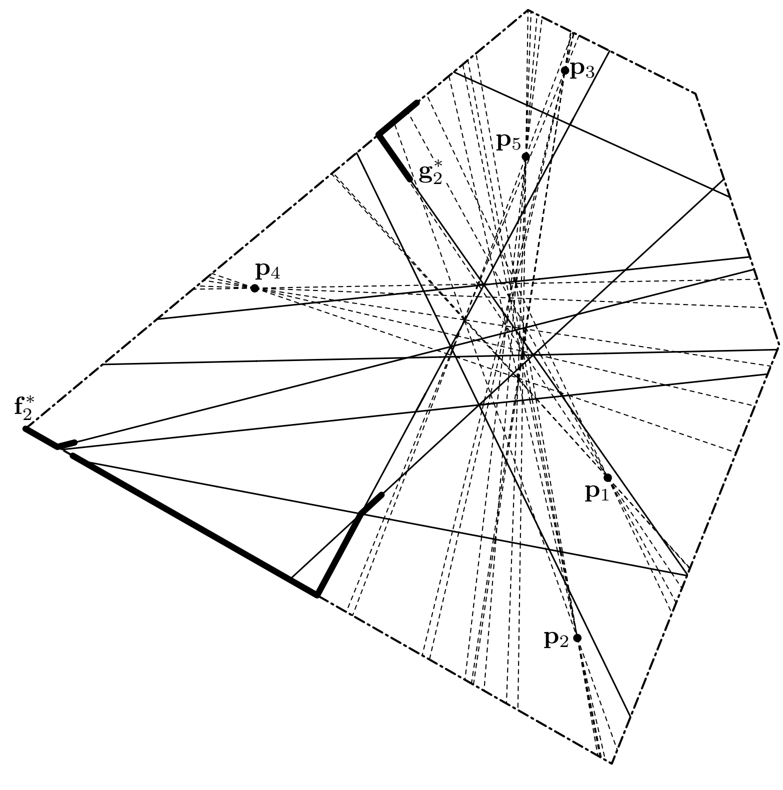

Figure 4: Pareto set for anticenter-maxion with partial covering criteria

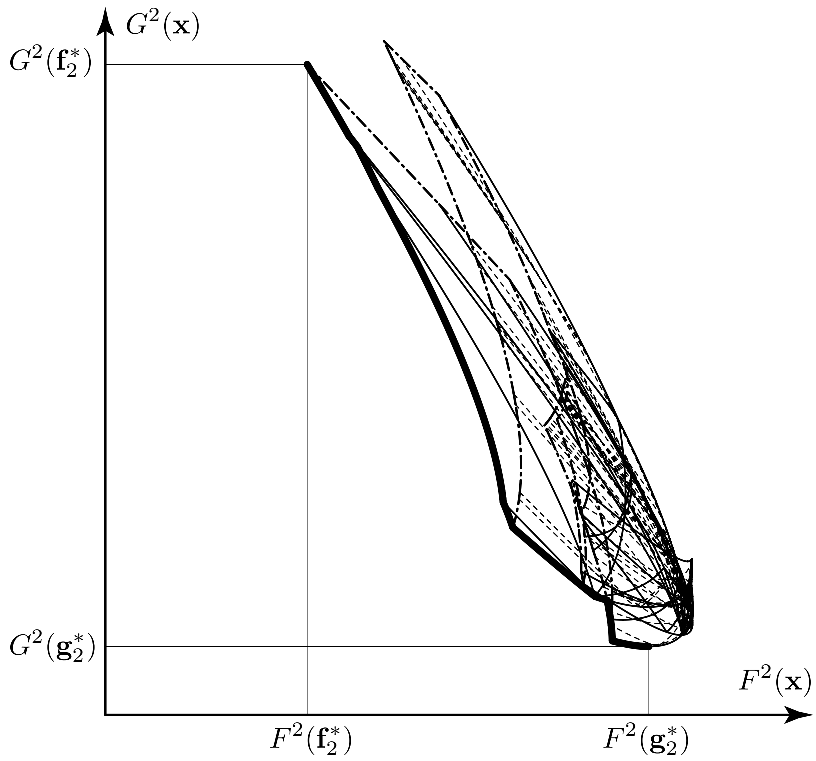

Figure 5: Trade-off curve for anticenter-maxion with partial covering criteria

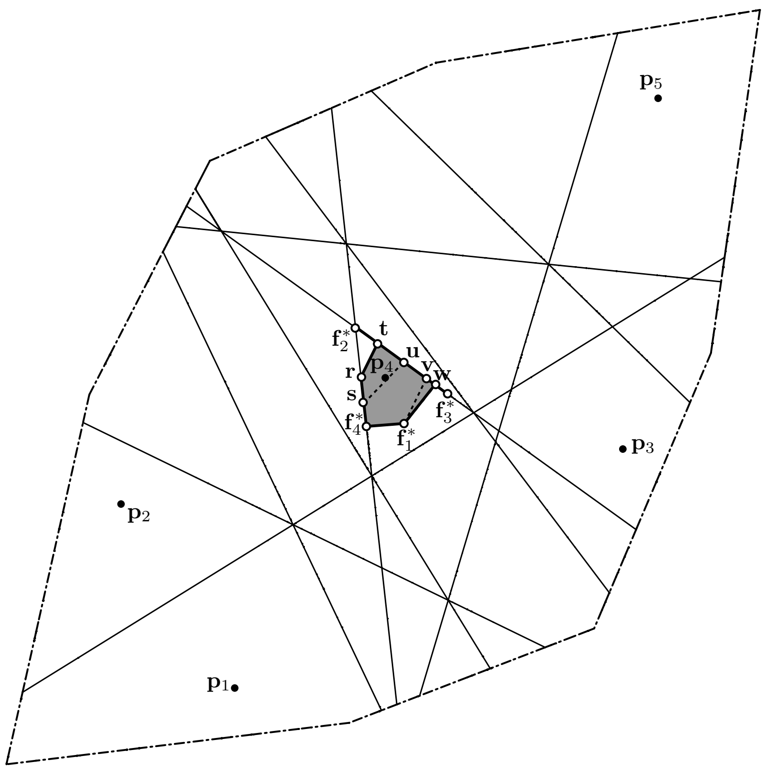

Figure 6: Pareto set for four-objective problem

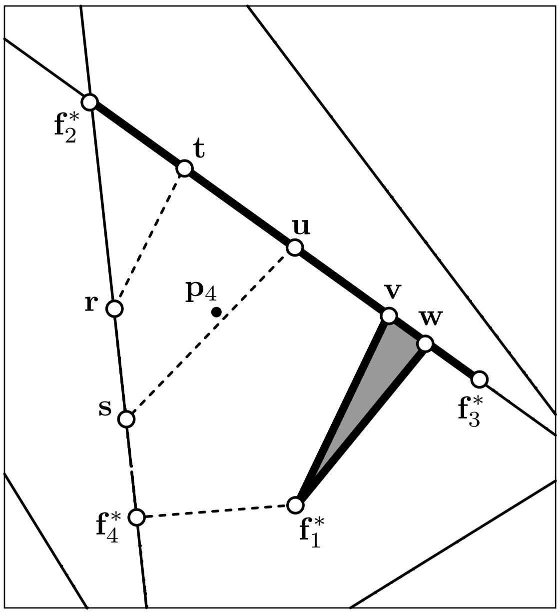

Figure 7: Pareto set E^*_{123}

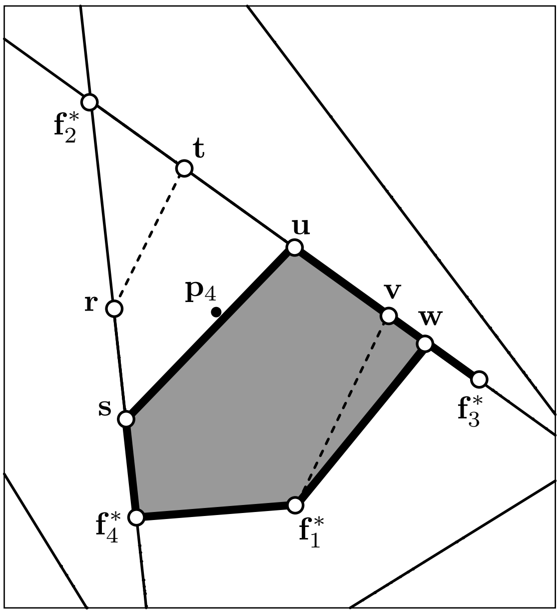

Figure 9: Pareto set E^*_{134}

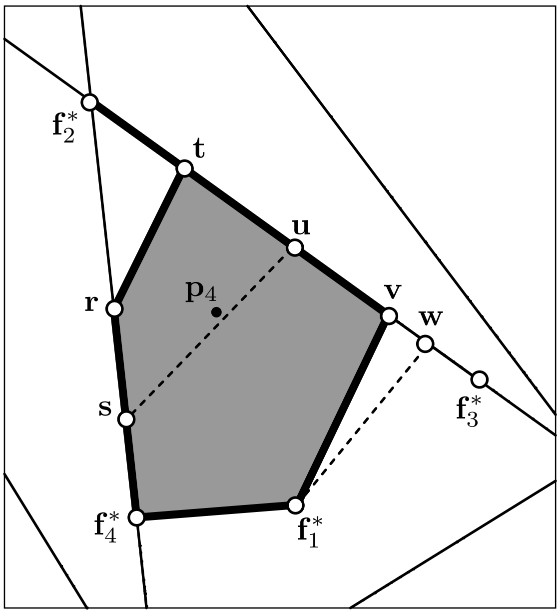

Figure 8: Pareto set E^*_{124}

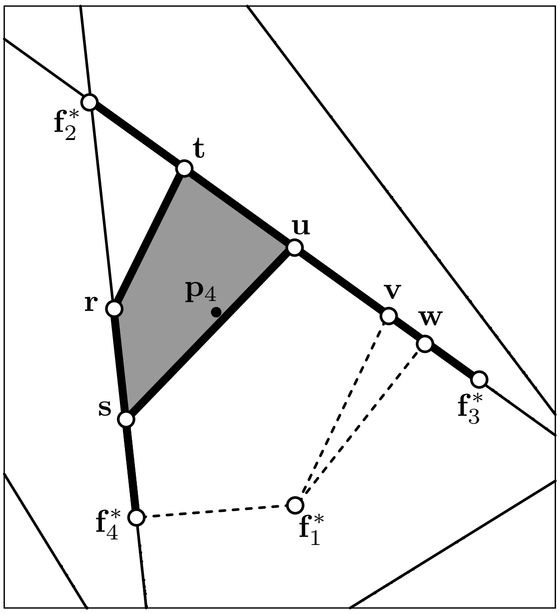

Figure 10: Pareto set E^*_{234}